Dynamic strain measurements in a sliding microstructured contact

2008 J. Phys.: Condens. Matter 20 015004

(http://iopscience.iop.org/0953-8984/20/1/015004)

J. Phys.: Condens. Matter **20** (2008) 015004 (7pp) doi:10.1088/0953-8984/20/01/015004

Dynamic strain measurements in a sliding microstructured contact

Roland Bennewitz[1], **Jonathan David, Charles-François de Lannoy, Benedict Drevniok, Paris Hubbard-Davis, Takashi Miura and Olga Trichtchenko**

Department of Physics, McGill University, Montreal, QC, H3A 2T8, Canada

E-mail: roland.bennewitz@mcgill.ca

Received 30 August 2007, in final form 26 October 2007
Published 5 December 2007
Online at stacks.iop.org/JPhysCM/20/015004

Abstract
A novel experiment is described which measures the tangential strain development across the contact between a PDMS (polydimethylsiloxane) block and a glass surface during the initial stages of sliding. The surface of the PDMS block has been microfabricated to take the form of a regular array of pyramidal tips at 20 μm separation. Tangential strain is measured by means of light scattering from the interface between the block and surface. Three phases are observed in all experiments: initial shear deformation of the whole PDMS block, a pre-sliding tangential compression of the tip array with stepwise increase of the compressive strain, and sliding in stick–slip movements as revealed by periodic variation of the strain. The stick–slip sliding between the regular tip array and the randomly rough counter surface always takes on the periodicity of the tip array. The fast slip can cause either a sudden increase or a sudden decrease in compressive strain.

1. Introduction

The transition from sticking to sliding in a laterally stressed contact is a process of great importance for tribology. It manifests itself in the difference between static and dynamic friction coefficients, a difference which is notoriously difficult to reproducibly measure and to quantitatively predict. The detachment of the contacting surfaces at the onset of sliding is a complex process which involves dynamic processes across the extended contact. Examples are Schallamach's detachment waves crossing the sliding contact between rubber and glass [1] or the shear cracks observed by Baumberger *et al* which facilitate the frictional dynamics of sliding gel/glass contacts [2]. Recent experimental studies have studied the dynamic processes at the onset of sliding by direct time-resolved measurements of the real area of contact [3–5]. Discontinuities in the contact dynamics do not only mark the onset of sliding but may also be manifest during sliding as stick–slip behavior. Stick-slip movement can simply be caused by the surface roughness. The relevant length scales are then revealed by a correlation analysis of the friction signal as shown by Rabinowicz [6]. Furthermore, stick–slip can be the expression of a time dependence of adhesion in multi-contact interfaces, as recently reviewed by Baumberger and Caroli [7]. For lubricated contacts, the time dependence can take the form of a phase transition between liquid-like and solid-like confined lubricants [8].

In this paper we study the onset of sliding between a polished glass surface and a micro-structured PDMS (polydimethylsiloxane) surface carrying a regular array of pyramidal tips. The tip array represents an extreme simplification of the multi-asperity nature of the contact between real surfaces, which determines their tribological properties [9]. Dürig *et al* have suggested that micro-fabricated tip arrays are a nanotribology testing ground for multi-asperity contacts when they studied tip arrays for their use as a mechanical data storage device [10]. The basic idea of using regular mesoscopic arrays for fundamental tribology studies has recently been realized with hexagonally arranged patches of vertically aligned carbon nanotubes [11]. Structured rubber surfaces with regularly arranged pillars of sub-millimeter spacing also show a great influence of the surface structure on adhesion, which has been found to be a function of the perimeter of the real contact area [12]. In our work the use of a regularly structured PDMS surface is motivated by the desire to study the role of roughness in friction on a simple model system. Furthermore, the regularity of the structure allows us to study tangential strain across the tip array by means of optical light scattering. Throughout this paper we will use

[1] Author to whom any correspondence should be addressed.

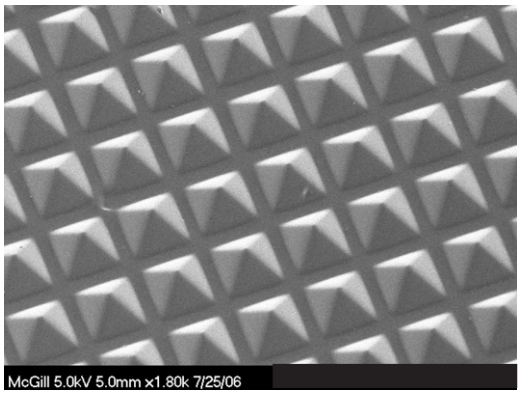

Figure 1. Scanning electron micrograph of the PDMS tip array. For imaging, the surface was covered with a thin gold film to avoid charging. The period of the array is 20 μm. The angle of view is tilted in order to visualize the three-dimensional structure of the surface.

the term compressive strain for tangential compressive strain across the contact, i.e. for a reduction of the average lateral distance between the regular features of our surface.

2. Experimental setup

2.1. Microfabrication of the tip arrays

The first step in the production of the PDMS tip arrays was the fabrication of a mould from a 6 inch silicon (100) wafer. The second step involves the curing of PDMS in the mould and the subsequent detachment of the tip arrays from the wafer.

For the production of the mould, a 1 μm thick oxide layer was grown on top of this wafer using a wet thermal oxidation process. The oxide was subsequently covered with a 1.4 μm thick layer of photoresist. A chrome-on-glass mask was created by printing a pattern on standard transparency paper, using a printer resolution of 5080 dpi, and transferring the pattern from the transparency to the mask. The pattern was an array of transparent squares with 50 μm side length each separated by 50 μm wide opaque stripes.

The photoresist was exposed to ultraviolet light through this mask using a stepper with a one fifth optical magnification factor. The photoresist was then developed and the oxide layer was patterned in a reactive ion etch. Finally, the residual photoresist was removed in a plasma asher. As a result, the oxide was removed in squares with a 10 μm side length, arranged in a rectangular array separated from one another by 20 μm. Pyramidal holes were etched into the silicon using the anisotropic etching rates of TMAH (tetramethylammonium hydroxide). In order to achieve a constant etch rate across the wafer, it was imperative that any native oxide layer be removed from the silicon surface by means of a short etch in hydrofluoric acid. This had to be done without removing the oxide pattern. The TMAH etch was stopped when the pyramids had formed. A final long etch with hydrofluoric acid removed the oxide pattern.

The PDMS (Sylgard 184) was mixed in a relation 10:1, poured over the silicon mould to a thickness of 2 mm, and cured at a temperature of 390 K. The PDMS film could be easily peeled from the mould in one piece. This could be achieved provided that the silicon mould had been rendered hydrophobic by a thorough cleaning in a mixture of sulphuric acid and hydrogen peroxide. Additionally, the mould had to be passivated in hydrofluoric acid immediately before the PDMS was poured into it. It was confirmed by scanning electron microscopy (SEM) that the PDMS tip array was not damaged during the peeling process, with the exception of an area of a few millimeters in width located at the rim of the sample. A SEM micrograph of the tip array can be found in figure 1.

2.2. Friction setup

A piece of PDMS (8.4 mm by 4.6 mm, 2 mm thickness) fully covered with tips (close to 100 000 in this area) was mounted on a brass block weighing 0.2 kg. The resultant average load was about 20 μN per tip. In order to attach the PDMS array to the brass block, the back side of the PDMS was first bonded to a glass slide by oxygen plasmation. The glass slide was then glued to the brass block.

The brass block is guided by an aluminum frame on a motorized translation stage. The aluminum frame is constructed to allow the brass block to smoothly slide vertically so that its weight could be applied as normal load to the contact area. Additionally, it is fashioned in such a way as to move the brass block horizontally without any tilt.

The counter surface is the upper face of a dove prism. This surface is optically polished to one half wavelength roughness. The goal of the experiment is to study strain across the tip array by means of scattering light. The beam of a HeNe laser (632.8 nm) enters the dove prism parallel to the top surface. The laser is refracted towards the top surface where it undergoes total internal reflection, and then refracted back to its original direction at the exit face of the prism (see figure 2). When the tip array comes into contact with the top surface of the prism, the evanescent field of

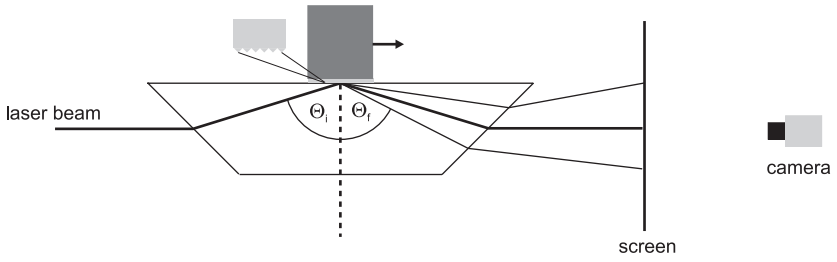

Figure 2. Schematic drawing of the experimental setup, the light beam propagation in the dove prism, and the notation of the angles used in the derivation.

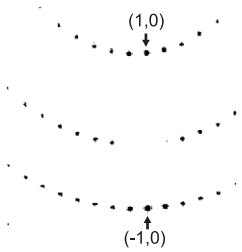

Figure 3. Light diffraction pattern for the unstrained tip array. The gray scale was inverted for better printing. The (1, 0) and (−1, 0) spots used for the analysis are labeled. The central (0, 0) spot has been blocked to avoid camera saturation.

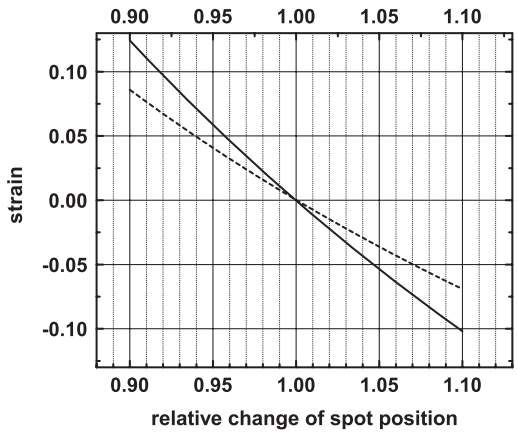

Figure 4. Strain versus distance between the (0, 0) spot and the (1, 0) and the (−1, 0) spots, respectively, on a screen far from the prism for the 20 μm tip array. The spot distances are normalized to the distance for the unstrained tip array.

the internally reflected light is disturbed. The total reflection is reduced at the points of tip–surface contact. Since this disturbance takes the form of a regular array, the reflected beam is diffracted. On a screen mounted in the far-field a diffraction pattern like the one presented in figure 3 can be observed. Note the symmetric curved distortion of the diffraction pattern which is characteristic for scattering in grazing incidence geometries as observed in reflection high-energy electron diffraction (RHEED), for example.

Any compressive strain in the tip array, i.e. a global decrease of the distance between tips in the course of sliding, manifests itself in an elongation of the diffraction pattern. Any decrease of order in the structure of the tip array, i.e. local changes in the distance between tips, manifests itself as a broadening of the diffraction spots.

The angles of diffraction inside the dove prism for the order of diffraction (q_1, q_2) are given by

$$\sin\Theta_f = \sqrt{\left(\sin\Theta_i + q_1\frac{\lambda}{a}\right)^2 + q_2^2\frac{\lambda^2}{a^2}}$$

$$\sin\phi_f = \frac{q_2\frac{\lambda}{a}}{\sin\Theta_f}.$$

In these formulas, a is the distance between tips, $\lambda = 632.8/n$ nm is the corrected wavelength in the medium with the index of refraction $n = 1.516\,89$, Θ is the angle of the light with respect to the surface normal, ϕ is the azimuthal angle of deflection of the outgoing light with respect to the direction of the incoming light. The angle of incidence for the internal reflection, Θ_i, is given by

$$\Theta_i = 45^\circ + \arcsin\left(\frac{\sin(45^\circ)}{n}\right) = 72.785^\circ.$$

The final result for the position of diffraction spots on the screen is a non-linear function of the tip distance a due to the non-linear diffraction of the light beams at the angled faces of the prism. Here, we limit the analysis to the relative change in position of the (1, 0) and the (−1, 0) spots with respect to the (0, 0) spot, which is plotted as a function of compressive strain in figure 4. For small values of the strain we can make a linear approximation: by measuring the relative change in distance of the (1, 0) and the (−1, 0) spots (labeled in figure 3) and multiplying the result by the average of the slopes in figure 4 at zero strain, we obtain a very good approximation for the strain in the tip array. The diffraction pattern and, thereby, the strain are recorded by means of a video camera at a rate of 30 frames per second.

3. Results

The load on the tip array is chosen such that most tips are in contact with the glass surface. Increasing the load starting from zero increases the intensity of the diffraction pattern. In these experiments the intensity of the diffraction pattern was just saturating, indicating that most tips were in contact with the glass prism.

As the PDMS block is made to slide across the glass prism, the diffraction pattern and thus the spacing between the tips is observed to change. The compressive strain in the tip array is calculated from the diffraction pattern and plotted against the distance that the translation stage travels. Throughout all the experiments we observe three consistently recurring subsequent phenomena. The three graphs in figure 5 show these recurring phases of motion for three different translation velocities. The graphs have been chosen to highlight detailed characteristics within the three overarching phases of motion. These phases are specified in the second graph of figure 5. The first phase (labeled I) is an initial flat, non-compressive phase. It is followed by (II) a considerable increase in the compressive strain, ending in a third phase (III) of rapid and periodic variation of the compressive strain around a constant value. Within each phase there are finer features which have been enlarged in each of the three graphs, and which will be discussed in detail.

Details for the position and the width of the diffraction spots are given in figure 6. The shift in the position of the spots during phase II (from A to B) is very large compared to their widths. The width can be observed to increase slightly upon compression. These profiles confirm that there is indeed a global average compression of the tip array and that spatial

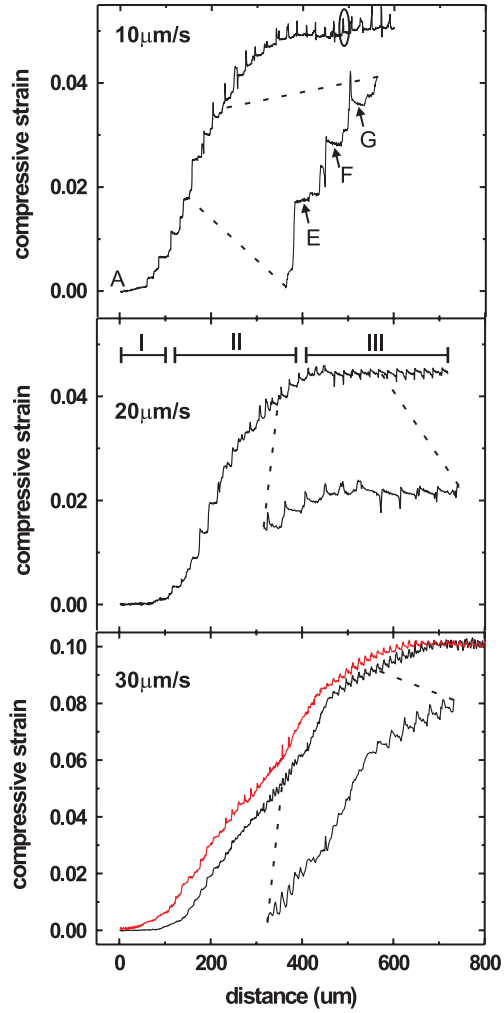

Figure 5. Compressive strain in the tip array versus distance traveled by the translation stage for velocities of 10, 20, and 30 μm s^{-1}, respectively. Three consistently recurring phases of motion are labeled I, II, and III (see text). Within each graph some characteristic features have been enlarged. The letters in the upper graph indicate the positions of diffraction spot profiles plotted in figure 6. The lower graph contains two results recorded in series starting from the same position of the glass surface after lifting the tip array off for relaxation of any remaining strain.

(This figure is in colour only in the electronic version)

variations in the strain across the tip array are small compared to the absolute value of the strain. The widths of the diffraction spots in figure 6 also allows us to determine the resolution of our experiment which is currently limited by the width of the light beam. The relative change in position of the diffraction spots can be measured to one tenth of their widths, i.e. to 0.002. Using the results in figure 4, this translates into a uncertainty of strain measurements of $\pm 0.24\%$.

No change at all is observed in the position of the lateral diffraction spots, i.e. the $(0, -1)$ and the $(0, 1)$ spots, upon sliding the tip array over the glass surface. We conclude that the tip array is not strained in the direction perpendicular to the sliding direction.

We assume that the three phases reflect the following processes: the first phase is due to a global shear deformation of the PDMS block with the tips sticking to their position on the glass surface, the second phase is a large tangential compression of the tip array as the tips begin sliding across the surface, and the final phase comprises stick–slip movement of the tip array. These three phases were consistently observed over a range of different experiments in which the parameters, i.e. sliding velocity, direction of motion, normal load, and spacing between the tips, were altered. In the following we will discuss the recurring phases in detail and describe the finer details within each phase. Additional phenomena that have occurred in certain experimental situations will also be briefly discussed.

3.1. Global shear deformation of the block

The initial stage of every sliding trial exhibits a region of seeming inactivity where nearly no change in strain occurs. This region has a consistent length on the order of 100 μm and is attributed to a shear deformation of the PDMS block. As the translation stage causes the brass block to move, the attached face of the PDMS block follows suit, however the tips in contact with the glass prism stick to its surface. The pliable tips shear in response to the motion and when they cease to shear, the block itself shears parallel to the prism in the direction of its motion. Figure 7(a) shows the tip array in its original configuration, and figure 7(b) the shear deformation at the end of the initial stage. The shear of the block changes neither the order of nor the spacing between the tips, which explains why the diffraction pattern does not change in this phase.

The PDMS block shears by approximately 5% before sliding, which is a strong but reasonable shear strain. The force required to shear the block by this amount can be calculated from the shear modulus G, and the shear strain $\Delta x/h = 5\%$ on the block as

$$F = G\frac{A\Delta x}{h}.$$

Assuming $G \sim 250$ kPa [13] and with the area of the PDMS block $A = 38.64$ mm^2 the amount of force required to shear the block is calculated to be 0.5 N, i.e. 5 μN per tip.

The end of this first phase marks the transition from a static contact area to the onset of pre-sliding events. This transitions occurs for a lateral force which is 0.25 of the normal force, where an error of 20% arises from the uncertainty of the shear modulus. The value of 0.25 is on the lower side of the kinetic friction coefficients found for dry PDMS friction on glass (0.2–0.5) [14, 15]. One has to keep in mind that it reflects the onset of pre-sliding rather than sliding and the particular roughness of the micro-structured PDMS surface. The static friction coefficient is dominated by the adhesion properties of the surface rather than hysteretic properties of the bulk and therefore depends strongly on the real contact area [16].

3.2. Compression of the tip array

Once the shear stress acting on the block overcomes the 0.5 N force threshold, the tip array partially begins sliding across the prism surface. In the initial stage of the motion the tip array

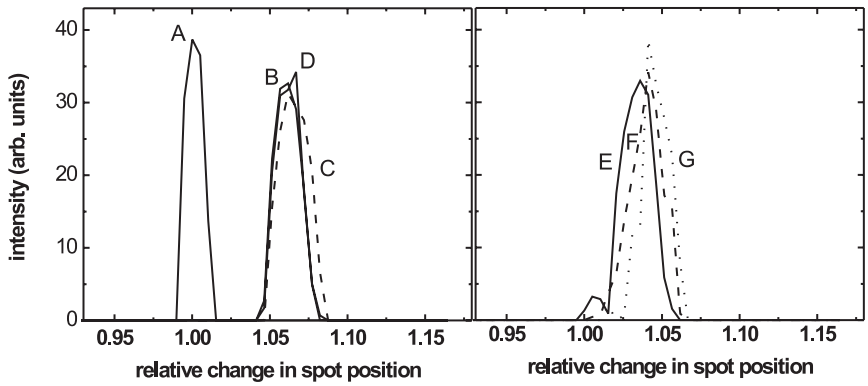

Figure 6. Profiles of the $(-1, 0)$ diffraction spots for several positions in the data set shown in the upper graph in figure 5. The labels indicate the position of each profile. Profile A represents the unstrained tip array. Profiles B, C, and D are, respectively, recorded directly before the slip, directly after the slip at highest compression, and after relaxation for the stick–slip event encircled in figure 5. Profiles E, F, and G are recorded on the compression steps indicated in the enlargements in the upper graph of figure 5.

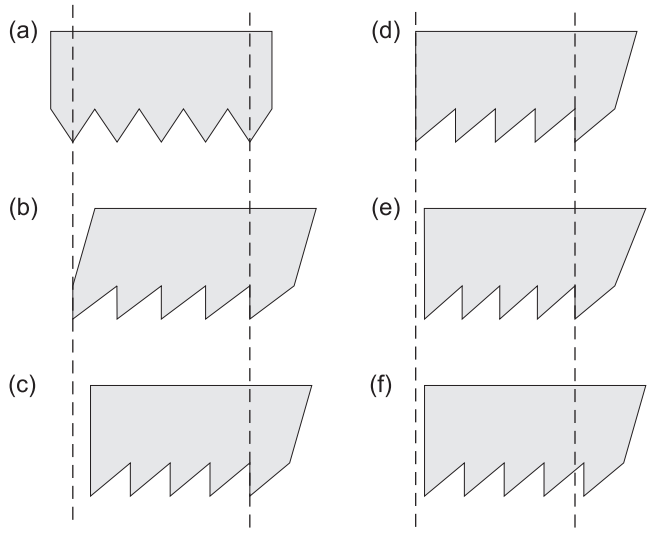

Figure 7. Schematic drawing of the strain development described in the text. Note that the drawings are far out of scale. (a) Original configuration of the tip array. (b) Configuration at the end of phase I; the PDMS block has undergone a global shear deformation, but the tips have still the same average distance, i.e. there is no tangential strain. (c) Configuration at the end of phase II; the average distance between tips is reduced, i.e. there is a tangential compressive strain across the contact. (d)–(f) Stick–slip motion as observed in phase III. In type I stick–slip the transition from (d) to (e) is a fast compression and that from (e) to (f) a slow relaxation. In type II stick–slip the transition from (d) to (e) is a slow increase of strain and that from (e) to (f) a fast relaxation.

undergoes a net tangential compressive strain which reaches values on the order of 5.0%. Throughout the experiments, we observed values of final compressive strain ranging from 4.0% to as high as 9.0%.

The compression of the tip array in phase II does not proceed continuously but in steps of varying width and height (see figure 5). The partial motion of the tip array and consequent build-up of strain occurs in quick movements followed by static episodes. The enlarged part of the lower graph indicates that for advanced compression the strain relaxes partially in between the sharp step-wise increases. The latter behavior marks the transition to the stick–slip movement described in section 3.3.

The profiles of the diffraction spots E, F, and G in figure 6 reflect the strain during the step-like compression in the pre-sliding regime in our experiment. They do not exhibit a significant increase in width. Any inhomogeneities or gradients in the strain across the contact would broaden the diffraction spots. We can conclude that the increasing tangential strain in this phase is quite homogeneous. Any lateral variations of the strain are small compared to the absolute value of the strain.

In the lower graph of figure 5 one can observe a change from a step-wise increase of strain to a stick–slip regime, back to step-like increase, and finally again to stick–slip movements. When repeating the experiment starting from the same position, the strain versus distance curves exhibit these changes again at very similar positions. This is a clear indication that local variations of the surface structure have an important influence on the development of tangential strain in the tip array. We will come back to the role of the surface structure when discussing the periodicity of stick–slip in section 3.3.

A possible scenario for the compression phase is that the trailing part of the tip array becomes unstuck from the glass before the leading part of the array. As these rear tips start moving, the rear of the PDMS block relaxes from the sheared angle to a relaxed position with respect to the attached upper face of the block, see figure 7(c). This relaxation causes a global decrease in the average distance between the tips, which we describe as a tangential compressive strain and observe as an increase in the distance between diffraction spots. The scenario is supported by the similarity of the values for the initial shear deformation of the PDMS block and the resulting compressive strain in the tip array. It is furthermore in agreement with observations by Schallamach [1] for sliding rubber/glass contacts and Baumberger *et al* [2] for gel/glass contacts. In their experiments detachment waves or shear cracks, respectively, nucleate at the trailing edge of the sliding elastomer. Our experiment does not allow to directly observe

whether the leading edge of the tip array is stuck to the surface in this phase or starts sliding like the trailing edge. However, the observation of an increasing homogeneous compressive strain proves that the trailing edge slides a larger distance than the leading edge.

This phase of step-wise build-up of strain falls into a category of pre-sliding also discussed by Rubinstein *et al* [5]. Rubinstein *et al* find frustrated crack-like precursors in the pre-sliding regime, which we think are also observed in our phase II of sliding as sudden increases in compressive strain. They show that these rapid crack-like precursors create large non-uniformities in the fractal contact area between two bodies that precondition the interface before sliding starts. The analysis of our results shows a homogeneous tangential strain across the contact. An explanation for the homogeneity of the strain may be the thinness of our PDMS sample with the unstrained upper side firmly bonded to the support. Furthermore, we expect a homogeneous frictional force acting across the contact, in contrast, for example, to the inhomogeneous strain due to a parabolically distributed lateral force in Schallamach's ball-on-plane experiments [1].

Rubinstein *et al* describe how eventually the propagation of a crack through the whole contact facilitates the transition to stick–slip sliding. We observe a more gradual transition from the step-wise increase of strain reflecting pre-sliding events to a very regular stick–slip sliding, which will be discussed in the following section.

3.3. Stick–slip motion in the tip array

The third phase of sliding motion exhibits periodic variations around a constant value of compressive strain, indicating a stick–slip process. Profiles B, C, and D in figure 6 describe the development of the strain during a stick–slip event. Profile C, taken directly after the slip, is wider than profiles B and D. This indicates that the slip creates a variation or a gradient of strain across the tip array which is subsequently relaxed.

The strain is observed to follow one of two patterns during the stick–slip movement, for which examples are given in figure 8. In the first pattern the strain increases considerably (by up to 0.5%) and rapidly (faster than 1/10 of a second, the actual time resolution of our camera) followed by a gradual relaxation, after which another sudden increase occurs. The second pattern is inverted with respect to the first. We observe a gradual increase in compressive strain until the tip array relaxes in a sudden step and then compresses slowly once again. The amount by which the array relaxes or compresses between slip events can be converted into local variations of the average distance between neighboring tips. For an increase of 0.5% in compressive strain, the distance between tips must be reduced on average by only 0.5% of 20 μm or 100 nm.

We believe that the two strain patterns shown in figure 8 arise from the same type of stick–slip behavior. Lateral force is built up by the continuous movement of the translation stage until the slip is initiated and the lateral force suddenly reduced. Our results show that the slip movement causes either a sudden increase or a sudden decrease the tangential strain. The situation is drawn in figures 7(d)–(f). For type I stick–slip, the compression from (d) to (e) happens in a sudden slip movement, while the relaxation from (e) to (f) occurs gradually. For type II stick–slip, the compression from (d) to (e) builds up gradually, and the relaxation from (e) to (f) happens in a sudden slip. The occurrence of the two distinct patterns of stick–slip can then be explained by a variation of the glass surface structure across the area in contact with the tip array. A more adhesive area under the rear of the tip array favors type I stick–slip by causing a gradual decrease of the compression, which will retain its average value in a sudden step when the rear part of the tip array slips to a new position. A more adhesive area under the leading part of the tip array on the other side will favor type II stick–slip. In the lower graph of figure 5 we find that the two types of strain pattern in stick–slip alternate. When we repeat the experiment starting from the same position we find the same type of stick–slip in the strain occurring at the same position on the glass surface. This finding confirms the crucial role of local variations of the roughness for the form of stick–slip movements. Variations of the surface structure are known to have a strong influence on the appearance of the stick–slip motion also on the macroscopic scale [17].

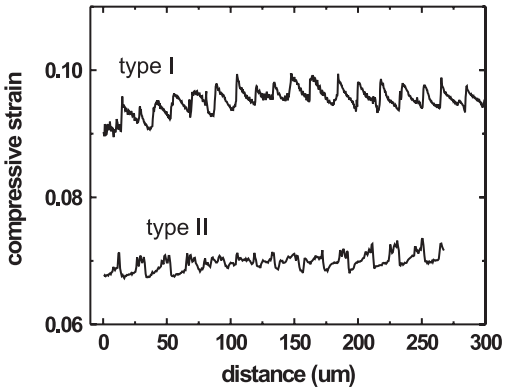

Figure 8. Two patterns of strain development during stick–slip movement as observed in the strain versus distance curves.

In all stick–slip movements observed in phase III, the periodicity of the stick–slip was very close to 20 μm, which is the original spacing between tips in the array. In order to confirm the relationship between the period of the stick–slip and the spacing between the tips, experiments were performed using an array with a tip spacing of 40 μm, which indeed exhibited stick–slip in intervals of 40 μm.

The roughness of the polished glass surface was specified to half wavelength, and the surface quality as 60/40 scratch and dig. On average we therefore expect a random surface roughness with all spatial frequencies and with height variations of the order of fractions of a micrometer, plus an occasional scratch with a width of up to 60 μm. Convoluting the shape of the 20 μm array with the random surface roughness yields a random structure with peaks every 20 μm. As the array slides across the glass prism, tips will stick in troughs or in front of peaks at random. However, should a group of tips come to stick at a set of troughs and peaks on the surface, there will be an increased probability that in a slip movement the line of tips will move forward by 20 μm and stick to the same set of surface obstacles. The result will be

a stick–slip sliding with the periodicity of the tip array. Our result is an confirmation of the original idea of Rabinowicz that characteristic length scales of the surface topography can be detected as a correlation in the kinetic friction [6], in our experiment in the dynamic strain. The stick–slip process does not fully relax the tip array, but occurs in a state of compressive strain across the tip array. This observation is in agreement with a report that the non-uniformity of the contact area does not recover during stick–slip motion [5].

3.4. Additional phenomena for reversed movement

The symmetry of the experiment with respect to the sliding direction was checked by comparing the strain development for forward and backward sliding starting from the same position. The essential result, i.e. the occurrence of the three phases in the development of compressive strain, were found to be independent of the sliding direction. On some occasions, however, we first observed a minor expansion of the tip array before the usual pattern of compression started to develop. We believe that in these cases the surface of the PDMS block has a small tilt with respect to the glass surface with a stronger contact at the trailing edge. As the translation stage starts to move, tips at the rear stick to the glass surface and the tip array is expanded. This expansion continues until the motion of the stage has compensated the tilt and the normal phases of compression start to develop.

We have also stopped the translation stage once sliding of the contact had developed, and reversed the direction of motion without releasing the strain. The compressive strain first rapidly decreased, and then a stick–slip motion in the opposite direction started as revealed by the typical periodic variation of the strain. The average compressive strain was typically lower after reversal of the sliding direction. However, the compressive strain never came close to zero, confirming that the compressed state of the tip array persists during the change of sliding direction.

4. Conclusion

In summary, we have introduced a novel experiment which measures the strain in the contact between a PDMS tip array and a polished glass surface at the onset of sliding. The inception of sliding is found to occur in three phases. First, the PDMS sample shears without changing the strain in the contact. In the second phase, a compressive strain is built up with values of typically 5%. Local variations in the strain across the tip array are small compared to the average strain. The compression mostly progresses in the form of step-like increases which are reminiscent of crack-like precursors to sliding. Finally, the contact starts to slide in a stick–slip movement which manifests itself as a periodic variation of the strain. The period of the stick–slip is always that of the regular tip array. We believe that the stick–slip originates in the random roughness of the glass surface and that its regularity arises from a convolution with the regular structure of the tip array. The periodic line of tips slips between the same set of troughs and peaks on the surface, thereby imposing its periodicity onto the stick–slip movement. A further indication that the surface roughness plays a pivotal role for the sliding is the observation that details in the appearance of the stick–slip variation reproducibly change for certain locations on the glass surface.

Acknowledgments

We would like to acknowledge the assistance of the McGill Microfabrication Laboratory (funded by CFI, NSERC and VRQ) in preparing the samples described here. The work was financially supported by NSERC and by an Undergraduate Research Award of the American Vacuum Society.

References

[1] Schallamach A 1972 *Wear* **17** 301
[2] Baumberger T, Caroli C and Ronsin O 2002 *Phys. Rev. Lett.* **88** 075509
[3] Rubinstein S, Cohen G and Fineberg J 2004 *Nature* **430** 1005
[4] Ovcharenko A, Halperin G, Etsion I and Varenberg M 2006 *Tribol. Lett.* **23** 55–63
[5] Rubinstein S M, Cohen G and Fineberg J 2007 *Phys. Rev. Lett.* **98** 226103
[6] Rabinowicz E 1956 *J. Appl. Phys.* **27** 131
[7] Baumberger T and Caroli C 2006 *Adv. Phys.* **55** 279348
[8] Yoshizawa H and Israelachvili J 1993 *J. Phys. C: Solid State Phys.* **97** 11300
[9] Bowden F and Tabor D 1986 *The Friction and Lubrication of Solids* (Oxford: Clarendon)
[10] Durig U, Cross G, Despont M, Drechsler U, Haberle W, Lutwyche M, Rothuizen H, Stutz R, Widmer R, Vettiger P, Binnig G, King W and Goodson K 2000 *Tribol. Lett.* **9** 25–32
[11] Lou J and Kim K S 2007 *Mater. Sci. Eng.* A at press (doi:10.1016/j.msea.2006.09.186)
[12] Varenberg M, Peressadko A, Gorb S and Arzt E 2006 *Appl. Phys. Lett.* **89** 121905
[13] Lötters J, Olthuis W, Veltink P and Bergveld P 1997 *J. Micromech. Microeng.* **7** 145–7
[14] Kaneko D, Oshikawa M, Yamaguchi T, Gong J P and Doi M 2007 *J. Phys. Soc. Japan* **76** 043601
[15] Tambe N and Bhushan B 2005 *Ultramicroscopy* **105** 238–47
[16] Persson B, Albohr O, Tartaglino U, Volokitin A and Tosatti E 2005 *J. Phys.: Condens. Matter* **17** R1–62
[17] Ma S and He C 2001 *Tectonophysics* **337** 135–45